energies

MDPI

Article

Growth Kinetics and Optical Properties of $CsPbBr_3$ Perovskite Nanocrystals

Sung Hun Kim [1], Kyoung-Duck Park [2] and Hong Seok Lee [1,*]

[1] Department of Physics, Research Institute of Physics and Chemistry, Jeonbuk National University, Jeonju 54896, Korea; kim940122@jbnu.ac.kr
[2] Department of Physics, Ulsan National Institute of Science and Technology (UNIST), Ulsan 44919, Korea; kdpark@unist.ac.kr
* Correspondence: hslee1@jbnu.ac.kr

Abstract: We synthesized $CsPbBr_3$ perovskite nanocrystals (NCs) at different reaction temperatures and tracked their growth kinetics on the basis of their optical properties and estimated size. The energies of the absorption and fluorescence (FL) peaks with increasing reaction temperature for the $CsPbBr_3$ perovskite NCs were tuned within the regions of 2.429–2.570 eV and 2.391–2.469 eV, respectively, depending on size of the NCs (9.9–12.5 nm). The Stokes shifts of $CsPbBr_3$ perovskite NCs with increasing NC size decreased from 101 meV to 38 meV. The full-width at half-maximum of the FL peaks for the CdSe NCs decreased from 150 meV to 90 meV because of the improved size uniformity of the $CsPbBr_3$ perovskite NCs. The energy spacing of $CsPbBr_3$ perovskite NCs synthesized at various reaction temperatures was calculated from Tauc plots; this information is critical for determining the bandgap energy and enables the size of the $CsPbBr_3$ perovskite NCs to be estimated using the effective mass approximation.

Keywords: perovskite nanocrystals; $CsPbBr_3$; growth kinetics; energy spacing; effective mass approximation

Citation: Kim, S.H.; Park, K.-D.; Lee, H.S. Growth Kinetics and Optical Properties of $CsPbBr_3$ Perovskite Nanocrystals. *Energies* **2021**, *14*, 275. https://doi.org/10.3390/en14020275

Received: 8 November 2020
Accepted: 5 January 2021
Published: 6 January 2021

1. Introduction

Lead halide perovskite nanocrystals (NCs) have inspired enormous interest in optoelectronics applications, such as light-emitting [1,2] and light-harvesting [3,4] devices and lasers [5], because of their tunable optical bandgaps through the precise engineering of halogen content and particle size [6]. In addition, nanostructured lead halide perovskites exhibit interesting optical properties, such as narrow photoluminescence (PL) linewidths and high PL quantum yields, enabling their potential application as high-performance optical materials [7]. In general, manipulating the defect concentration and size distribution of inorganic halide perovskite nanocrystals (IPNCs) is important for achieving narrow band emissions that improve color purity [8]. Because the high defect tolerance and self-passivating effect of IPNCs, the influence of defects on their optical properties is inconsequential compared with the influence of size homogeneity [9,10]. The surface-area-to-volume ratio of a material increases with decreasing particle size; below a certain particle size, surface ligands of a nanomaterial critically influence its photophysical properties, such as luminescence and carrier transport behavior [11]. During the synthesis of IPNCs, chemical agents that improve the dispersion stability and manipulate growth kinetics are added as fundamental components. Oleic acid and oleylamine are the most widely used surfactants in the ligand-assisted synthesis of $CsPbBr_3$ perovskite NCs [12]. Amines enhance the crystallization kinetics, potentially enabling the size tuning of perovskite NCs, whereas oleic acid plays a critical role in impeding NC aggregation and leads to stable NC colloids [13]. In the case of $CsPbX_3$, in particular, its bandgap cannot only be engineered through manipulation of its composition but also tuned via the reaction temperature. $CsPbBr_3$ perovskites are direct-bandgap structures with various crystal phases (e.g., orthorhombic, tetragonal, and

cubic crystal phases) [14]. However, only a few studies have focused on the temperature dependence of the photophysical properties of all-inorganic perovskites [15].

In this work, we investigated the growth kinetics and optical properties of $CsPbBr_3$ perovskite NCs with different reaction temperatures. $CsPbBr_3$ perovskite NCs synthesized at various reaction temperatures display size-tunability of their optical bandgap energies in the blue–green spectral range. The fluorescence (FL) of $CsPbBr_3$ perovskite NCs is characterized by narrow emission linewidths in the range of 90–150 meV. Moreover, from the physical parameters of $CsPbBr_3$, the radius of $CsPbBr_3$ perovskite NCs can be estimated on the basis of the effective mass approximation (EMA), which is used here to determine the energy spacing of the $CsPbBr_3$ perovskite NCs prepared at different reaction temperatures.

2. Materials and Methods

The $CsPbBr_3$ perovskite NCs were prepared at various reaction temperatures using a facile hot-injection method. Briefly, for the preparation of cesium oleate precursors, $CsCO_3$ (0.391 g, 1.2 mmol), oleic acid (1.27 mL, 4 mmol), and 1-octadecene (18.73 mL) were loaded into a 100 mL three-neck flask, dried at 120 °C for 1 h, and then heated under N_2 to 160 °C. After $CsCO_3$ was completely reacted with oleic acid, the mixture was preheated to 100 °C before injection. For the synthesis of $CsPbBr_3$ perovskite NCs, $PbBr_2$ (0.149 g, 0.4 mmol) and 1-octadecene (24 mL) were mixed in a 100 mL three-neck flask and dried for 1 h at 120 °C under vacuum. Oleic acid (1 mL) and oleylamine (3 mL) were injected at 120 °C under N_2. After the $PbBr_2$ salt was completely solubilized, the temperature was raised to the injection temperature (100–180 °C) to tune the size of the NCs and the pre-prepared Cs-oleate solution was quickly injected. After 5 s, $CsPbBr_3$ perovskite NCs were extracted and quickly cooled in an ice-water bath. The resultant NCs were precipitated by adding 5:1 (*v:v*) *tert*-butanol to a NC solution and centrifuging the mixture at 7000 rpm for 10 min; the supernatant was discarded, and the NCs were dispersed in toluene. The UV–vis absorption spectra and fluorescence spectra were recorded with a FLAME-S spectrometer (Ocean Optics Inc., Largo, FL, USA).

3. Results and Discussion

Figure 1a shows a schematic illustration of the hot injection method used to synthesize $CsPbBr_3$ perovskite NCs and an energy band diagram of different-sized NCs with increasing reaction temperature. This method is useful in colloidal synthesis strategy and can be adapted to synthesize various compound, semiconductor NCs. The growth kinetics of $CsPbBr_3$ perovskite NCs by the hot injection method follows the LaMer nucleation and growth mechanism [8]. The larger-sized perovskite NCs synthesized at the higher reaction temperature, which is a crucial factor to determine the morphology in the procedure of nucleation and growth of perovskite NCs, exhibit a smaller bandgap energy than that of the smaller-sized perovskite NCs [15]. Figure 1b shows the FL and absorption spectra of $CsPbBr_3$ perovskite NCs prepared at various reaction temperatures (100–180 °C) and at a reaction time of 5 s. The absorption and FL peaks of the $CsPbBr_3$ perovskite NCs show a band-edge red shift with increasing reaction temperature from 100 °C to 180 °C. Prior to quantitative analysis of emission spectra, the FL spectra measured in a wavelength scale are converted to an energy scale by using the Jacobian transformation [16]. The FL peaks of the as-obtained $CsPbBr_3$ perovskite NCs prepared at 100 °C, 120 °C, 140 °C, 160 °C, and 180 °C were located at 2.469 eV (502.3 nm), 2.440 eV (508.2 nm), 2.427 eV (510.9 nm), 2.405 eV (515.5 nm), and 2.391 eV (518.6 nm), respectively. When the synthesis temperature was greater than 120 °C, the first excitonic absorption peak broadened because of the formation of a population of larger particles [17]. In the spectrum of the sample prepared at the lowest reaction temperature (100 °C), the FL peak is asymmetric because of incomplete chemical reaction [17]. This behavior is attributed to the presence of a pool of monomers resulting from dissolution of particles with a radius less than the critical radius [18].

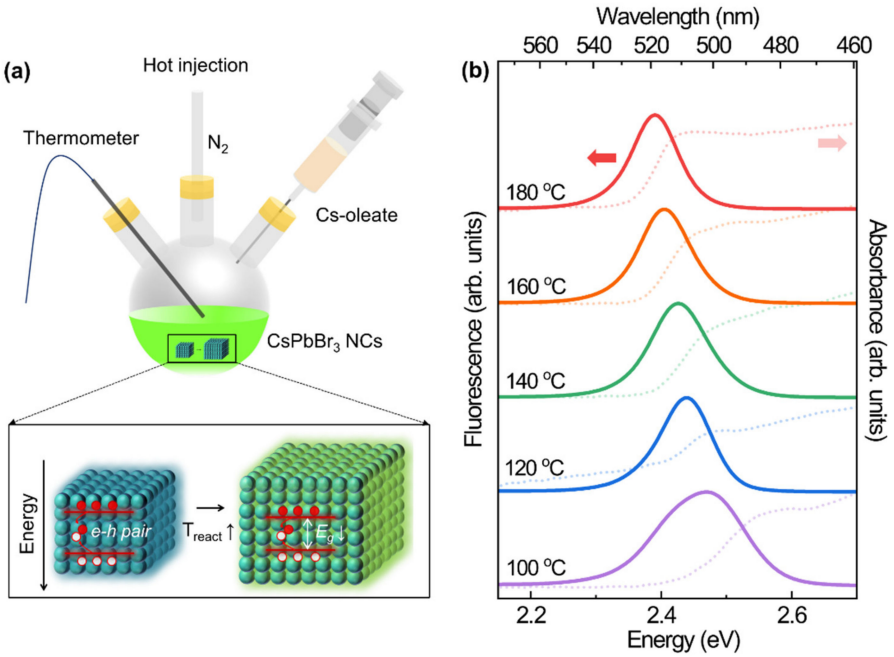

Figure 1. Synthesis and the optical properties of $CsPbBr_3$ perovskite nanocrystals (NCs): (**a**) Schematic illustration of the hot injection method and band diagram within different-sized $CsPbBr_3$ NCs; (**b**) absorption and fluorescence spectra for the $CsPbBr_3$ perovskite NCs prepared at different reaction temperatures.

Figure 2a shows the absorption and FL peak positions of $CsPbBr_3$ perovskite NCs prepared at different reaction temperatures. The absorption and FL peaks of the $CsPbBr_3$ perovskite NCs could be tuned in the regions of 2.429–2.570 eV and 2.391–2.469 eV, respectively. The absorption and FL peak positions for the perovskite NCs decreased with increasing reaction temperature because of an increase in the NC size [1,19,20]. In the plots of peak positions for the absorption and FL spectra, the reaction's temperature-dependent Stokes shift is observed due to the different size of synthesized $CsPbBr_3$ perovskite NCs. The Stokes shifts decreased from 101 meV to 38 meV with increasing NC size. The occurrence of the Stokes shifts is related to the crystal phase, NC size, and defect type [21]. Figure 2b shows the full-width at half-maximum (FWHM) of the FL peaks of the $CsPbBr_3$ perovskite NCs prepared at different temperatures. The FWHM of the FL peaks decreased from 150 meV to 90 meV with increasing reaction temperature because higher temperatures result in a narrower size distribution [18]. Thus, high reaction temperatures lead to rapid diffusion of the monomers and enabled the synthesis of high-quality $CsPbBr_3$ perovskite NCs with good size uniformity [2,12,18]. Figure 2c shows the photoluminescence quantum yield (PLQY) of $CsPbBr_3$ perovskite NCs as a function of reaction temperature. The relative PLQYs of the $CsPbBr_3$ perovskite NCs prepared at different reaction temperatures were determined by comparing the integrated emission of the NC samples with a standard fluorescence dye (Coumarin 500 in ethanol, QY = 47%). The highest PLQY of 56% was obtained for NCs prepared at the reaction temperature (140 °C).

Figure 3 shows Tauc plots for the $CsPbBr_3$ perovskite NCs prepared at different temperatures. The shape of the absorption edge in the absorption spectra of the $CsPbBr_3$ perovskite NCs is related to electronic transitions in the band-edge region [22]. The optical bandgap of the $CsPbBr_3$ perovskite NCs was calculated from the Tauc plots, which are valuable for determining the bandgap energy. The absorption coefficient (α), which is directly proportional to the optical density and incident photon energy ($h\nu$), can be used to determine the optical bandgap by extrapolating the straight-line portion of the plot of the quantity $(\alpha h\nu)^2$ vs. photon energy [22]. The authors of a previous study reported that the calculated bandgap of perovskite materials from the Tauc plot compares with the discrete Fourier transform computed bandgaps [23]. In addition, the bandgap can be estimated

using the Tauc plot without considering the exciton binding energy, and the results were in good agreement with the energy levels (conduction/valence band) derived from the photoelectron spectroscopy measurement [24]. The $CsPbBr_3$ perovskite NCs prepared under different reaction temperatures had an optical bandgap of 2.383–2.462 eV, and their optical bandgap decreased with increasing reaction temperature.

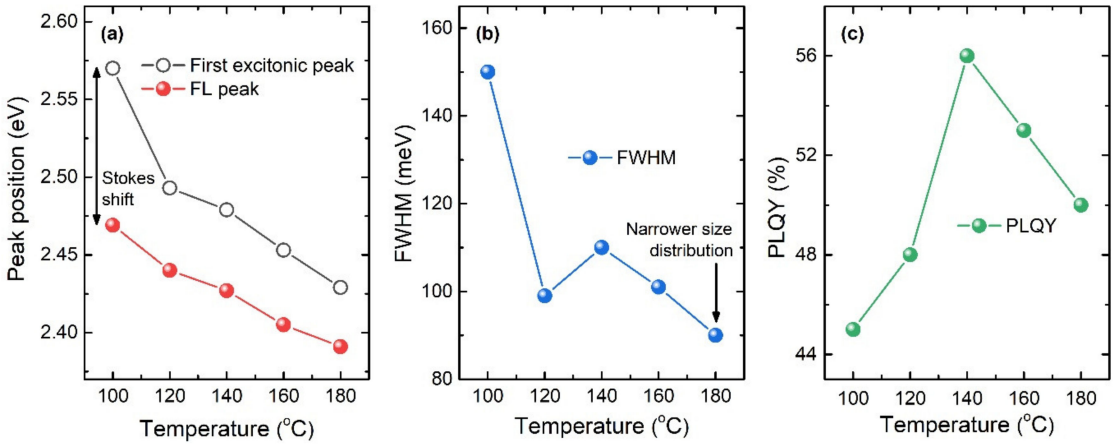

Figure 2. Optical analysis of $CsPbBr_3$ perovskite NCs as a function of reaction temperature: (**a**) Fluorescence and first excitonic absorption peak positions; (**b**) full-width at half-maximums (FWHMs); (**c**) photoluminescence quantum yield (PLQYs).

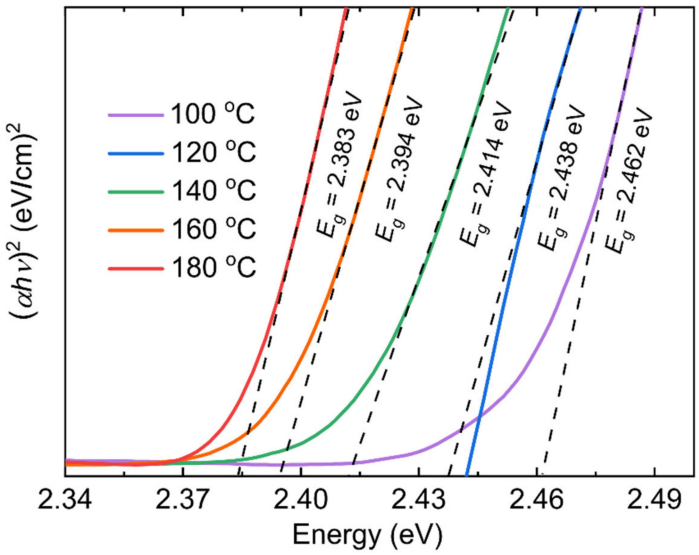

Figure 3. Optical bandgap of $CsPbBr_3$ perovskite NCs prepared at different reaction temperatures. Dashed lines indicate optical bandgaps determined from Tauc plots.

Figure 4 shows the calculated radius of the $CsPbBr_3$ perovskite NCs prepared at different temperatures, as determined using the EMA. The digital photographs of $CsPbBr_3$ perovskite NCs at different temperatures (100 °C, 140 °C, and 180 °C) under a single 365 nm UV light source are shown in the inset of Figure 4. In this EMA, an exciton is considered to be confined to a spherical crystallite and the mass of the electron and hole is substituted as the effective mass to define the wave function [25]. Equation (1) indicates the energy spacing (ΔE) of the $CsPbBr_3$ perovskite NCs prepared at different temperatures, as determined using the EMA [3,6]:

$$\Delta E = E_g - E_{bulk} = \frac{h^2}{8m^* r^2} = \frac{h^2}{8r^2}\left(\frac{1}{m_e^*} + \frac{1}{m_h^*}\right) \quad (1)$$

where E_g is the bandgap energy obtained from the Tauc plot of the $CsPbBr_3$ perovskite NCs, E_{bulk} is the bandgap energy of the bulk semiconductor, m *is the reduced mass of the exciton, m_e* is the effective mass of an excited electron, m_h* is the effective mass of an excited hole, r is the NC radius, and h is Planck's constant. The fitting of the energy spacing as a function of the radius for the $CsPbBr_3$ perovskite NCs prepared at different temperatures was obtained using the following parameters: E_{bulk} = 2.25 eV, m_e* = 0.15 eV, and m_h* = 0.14 eV [6]. The bandgaps are considered to reflect a constant offset of ~0.2 eV with respect to values measured experimentally at room temperature [6]. For a colloidal semiconductor NC to exhibit quantum-dot-like behavior, the NC diameter must be similar to or less than that of the exciton Bohr diameter, a_0 [25]. This approximation provides an estimate for the shifts of the emission and first excitonic absorption peaks, which are in good agreement with the experimental observations.

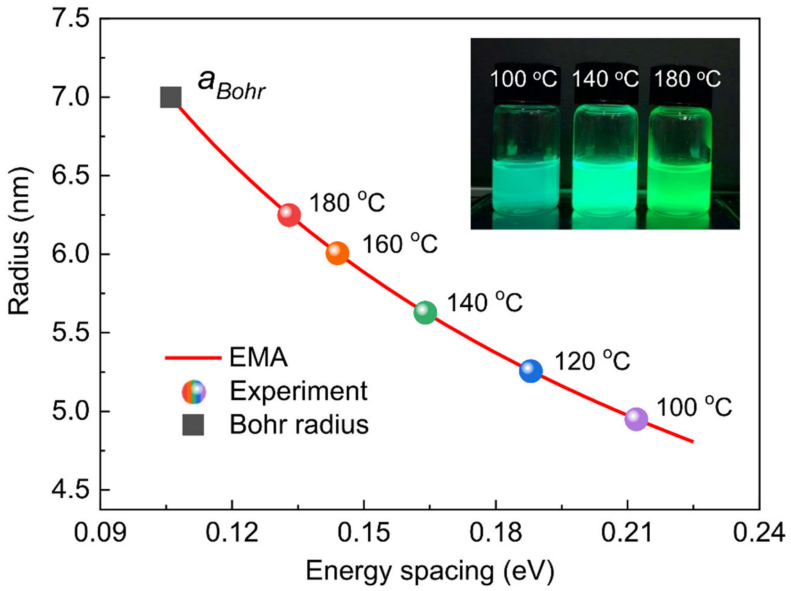

Figure 4. Calculated radius for $CsPbBr_3$ perovskite NCs as a function of the energy spacing. The experimental data are plotted with symbols and the solid line represents theoretical prediction (effective mass approximation, EMA).

The energy spacing of the $CsPbBr_3$ perovskite NCs was calculated from their Tauc plots, and their diameters were estimated using the EMA. Table 1 shows the values for the energy spacing and diameter of $CsPbBr_3$ perovskite NCs that yield the best fit of the experimental data to Equation (1); the fitted curve is included in Figure 4. The size of $CsPbBr_3$ perovskite NCs with increasing reaction temperature increased due to a decrease in the energy spacing resulting from a decrease in the optical bandgap of NCs. The diameter of the $CsPbBr_3$ perovskite NCs ranged from 9.9 nm to 12.5 nm. These results are in agreement with the transmission electron microscopy observations of $CsPbBr_3$ perovskite NCs reported by Protesescu et al. [6].

Table 1. Energy spacing and diameter for $CsPbBr_3$ perovskite NCs prepared at different reaction temperatures.

Reaction Temperature (°C)	100	120	140	160	180
Energy Spacing (eV)	0.21	0.19	0.16	0.14	0.13
Diameter (nm)	9.9	10.5	11.3	12.0	12.5

4. Conclusions

We characterized the size dependence of the optical properties and the energy spacing of $CsPbBr_3$ perovskite NCs prepared at various reaction temperatures. With increasing size

of the $CsPbBr_3$ perovskite NCs, band-edge red shifts occurred in their absorption and FL spectra. With increasing size of the $CsPbBr_3$ perovskite NCs, their Stokes shifts decreased from 101 meV to 38 meV. The FWHM of the FL peaks for the $CsPbBr_3$ perovskite NCs decreased from 150 meV to 90 meV because of the NCs' narrower size distribution when prepared at higher temperatures. The size of the $CsPbBr_3$ perovskite NCs was estimated using Tauc plots and the EMA. The results presented here improve the understanding of the growth kinetics and photophysics of $CsPbBr_3$ perovskite NCs and help in the development of high efficiency optoelectronic devices.

Author Contributions: Conceptualization, S.H.K. and H.S.L.; methodology, S.H.K.; validation, S.H.K., K.-D.P., and H.S.L.; formal analysis, S.H.K.; data curation, S.H.K. and K.-D.P.; writing—original draft preparation, S.H.K.; writing—review and editing, K.-D.P. and H.S.L.; visualization, K.-D.P.; supervision, H.S.L.; project administration, H.S.L.; funding acquisition, H.S.L. All authors have read and agreed to the published version of the manuscript.

Funding: This research was supported by the Basic Science Research Program through the National Research Foundation of Korea (NRF) funded by the Ministry of Science and ICT (NRF-2018R1A2B6001019) and "Research Base Construction Fund Support Program" funded by Jeonbuk National University in 2020.

Institutional Review Board Statement: Not applicable.

Informed Consent Statement: Not applicable.

Data Availability Statement: Data is contained within the article.

Conflicts of Interest: The authors declare no conflict of interest.

References

1. Song, J.; Li, J.; Li, X.; Xu, L.; Dong, Y.; Zeng, H. Quantum dot light-emitting diodes based on inorganic perovskite cesium lead halides ($CsPbX_3$). *Adv. Mater.* **2015**, *27*, 7162–7167. [CrossRef] [PubMed]
2. Li, X.; Wu, Y.; Zhang, S.; Cai, B.; Gu, Y.; Song, J.; Zeng, H. $CsPbX_3$ quantum dots for lighting and displays: Room-temperature synthesis, photoluminescence superiorities, underlying origins and white light-emitting diodes. *Adv. Funct. Mater.* **2016**, *26*, 2435–2445. [CrossRef]
3. Li, X.; Cao, F.; Yu, D.; Chen, J.; Sun, Z.; Shen, Y.; Zhu, Y.; Wang, L.; Wei, Y.; Wu, Y.; et al. All inorganic halide perovskites nanosystem: Synthesis, structural features, optical properties and optoelectronic applications. *Small* **2017**, *13*, 1603996. [CrossRef] [PubMed]
4. Hoffman, J.B.; Zaiats, G.; Wappes, I.; Kamat, P.V. $CsPbBr_3$ solar cells: Controlled film growth through layer-by-layer quantum dot deposition. *Chem. Mater.* **2017**, *29*, 9767–9774. [CrossRef]
5. Wang, Y.; Li, X.; Song, J.; Xiao, L.; Zeng, H.; Sun, H. All-inorganic colloidal perovskite quantum dots: A new class of lasing materials with favorable characteristics. *Adv. Mater.* **2015**, *27*, 7101–7108. [CrossRef] [PubMed]
6. Protesescu, L.; Yakunin, S.; Bodnarchuk, M.I.; Krieg, F.; Caputo, R.; Hendon, C.H.; Yang, R.X.; Walsh, A.; Kovalenko, M.V. Nanocrystals of cesium lead halide perovskites ($CsPbX_3$, X = Cl, Br, and I): Novel optoelectronic materials showing bright emission with wide color gamut. *Nano Lett.* **2015**, *15*, 3692–3696. [CrossRef] [PubMed]
7. Zhu, B.-S.; Li, H.-Z.; Ge, J.; Li, H.-D.; Yin, Y.-C.; Wang, K.-H.; Chen, C.; Yao, J.-S.; Zhang, Q.; Yao, H.-B. Room temperature precipitated dual phase $CsPbBr_3$–$CsPb_2Br_5$ nanocrystals for stable perovskite light emitting diodes. *Nanoscale* **2018**, *10*, 19262–19271. [CrossRef]
8. Li, X.; Zhang, K.; Li, J.; Chen, J.; Wu, Y.; Liu, K.; Song, J.; Zeng, H. Heterogeneous nucleation toward polar-solvent-free, fast, and one-pot synthesis of highly uniform perovskite quantum dots for wider color gamut display. *Adv. Mater. Interfaces* **2018**, *5*, 1800010. [CrossRef]
9. Huang, H.; Bodnarchuk, M.I.; Kershaw, S.V.; Kovalenko, M.V.; Rogach, A.L. Lead halide perovskite nanocrystals in the research spotlight: Stability and defect tolerance. *ACS Energy Lett.* **2017**, *2*, 2071–2083. [CrossRef]
10. Kang, J.; Wang, L.-W. High defect tolerance in lead halide perovskite $CsPbBr_3$. *J. Phys. Chem. Lett.* **2017**, *8*, 489–493. [CrossRef]
11. Li, X.; Yu, D.; Cao, F.; Gu, Y.; Wei, Y.; Wu, Y.; Song, J.; Zeng, H. Healing all-inorganic perovskite films via recyclable dissolution–recyrstallization for compact and smooth carrier channels of optoelectronic devices with high stability. *Adv. Funct. Mater.* **2016**, *26*, 5903–5912. [CrossRef]
12. Xia, H.; Wu, S.; Li, L.; Zhang, S. High binding ability ligand controlled formation of $CsPbX_3$ (X = Cl/Br, Br, I) perovskite nanocrystals with high quantum yields and enhanced stability. *RSC Adv.* **2018**, *8*, 35973–35980. [CrossRef]
13. Huang, H.; Susha, A.S.; Kershaw, S.V.; Hung, T.F.; Rogach, A.L. Control of emission color of high quantum yield $CH_3NH_3PbBr_3$ perovskite quantum dots by precipitation temperature. *Adv. Sci.* **2015**, *2*, 1500194. [CrossRef]
14. Zhang, X.; Xu, B.; Zhang, J.; Gao, Y.; Zheng, Y.; Wang, K.; Sun, X.W. All-inorganic perovskite nanocrystals for high-efficiency light emitting diodes: Dual-phase $CsPbBr_3$-$CsPb_2Br_5$ composites. *Adv. Funct. Mater.* **2016**, *26*, 4595–4600. [CrossRef]

15. Chen, C.; Zhang, L.; Shi, T.; Liao, G.; Tang, Z. Controllable synthesis of all inorganic lead halide Perovskite nanocrystals with various appearances in multiligand reaction system. *Nanomaterials* **2019**, *9*, 1751. [CrossRef] [PubMed]
16. Mooney, J.; Kambhampati, P. Get the basics right: Jacobian conversion of wavelength and energy scales for quantitative analysis of emission spectra. *J. Phys. Chem. Lett.* **2013**, *4*, 3316–3318. [CrossRef]
17. Lan, J.; Luo, L.; Wang, M.; Li, F.; Wu, X.; Wang, F. One pot gram-scale synthesis of $CsPbBr_3$ nanocrystals and their application in green LED. *J. Lumin.* **2019**, *210*, 464–471. [CrossRef]
18. Koolyk, M.; Amgar, D.; Aharon, S.; Etgar, L. Kinetics of cesium lead halide perovskite nanoparticle growth; focusing and de-focusing of size distribution. *Nanoscale* **2016**, *8*, 6403–6409. [CrossRef]
19. Kim, S.H.; Man, M.T.; Lee, J.W.; Park, K.-D.; Lee, H.S. Influence of size and shape anisotropy on optical properties of CdSe quantum dots. *Nanomaterials* **2020**, *10*, 1589. [CrossRef]
20. Kim, S.H.; Man, M.T.; Lee, H.S. Size and shell effects on CdSe quantum dots in binary ligand system. *Appl. Sci. Converg. Technol.* **2020**, *29*, 87–90. [CrossRef]
21. Brennan, M.C.; Herr, J.E.; Nguyen-Beck, T.S.; Zinna, J.; Draguta, S.; Rouvimov, S.; Parkhill, J.; Kuno, M. Origin of the size-dependent stokes shift in $CsPbBr_3$ perovskite nanocrystals. *J. Am. Chem. Soc.* **2017**, *139*, 12201–12208. [CrossRef] [PubMed]
22. Campos-Gonzalez, E.; Rodriguez-Fragozo, P.; de la Cruz, G.G.; Santoyo-Salazar, J.; Zelaya-Angel, O. Synthesis of CdSe nanoparticles immersed in an organic matrix of amylopectin by means of rf sputtering. *J. Cryst. Growth* **2012**, *338*, 251–255. [CrossRef]
23. Dutta, J.; Ajith, M.C.; Dutta, S.; Kadhane, U.R.; Kochupurackal, J.B.; Rai, B. An inherent instability study using ab initio computational methods and experimental validation of $Pb(SCN)_2$ based perovskites for solar cell applications. *Sci. Rep.* **2020**, *10*, 15241. [CrossRef]
24. Pan, J.; Quan, L.N.; Zhao, Y.; Peng, W.; Murali, B.; Sarmah, S.P.; Yuan, M.; Sinatra, L.; Alyami, N.M.; Liu, J.; et al. Highly efficient perovskite-quantum-dot light-emitting diodes by surface engineering. *Adv. Mater.* **2016**, *28*, 8718–8725. [CrossRef] [PubMed]
25. Chukwuocha, E.O.; Onyeaju, M.C.; Harry, T.S.T. Theoretical studies on the effect of confinement on quantum dots using the Brus Equation. *World J. Condens. Matter Phys.* **2012**, *2*, 96–100. [CrossRef]